Research Square

Preprints are preliminary reports that have not undergone peer review.
They should not be considered conclusive, used to inform clinical practice,
or referenced by the media as validated information.

The role of lacrimal gland quantitative parameters in orbital SPECT/CT-MRI for evaluating thyroid eye disease

Lixin Sun
Beijing Luhe Hospital, Capital Medical University
Xin Ma
Beijing Luhe Hospital, Capital Medical University
Lichun Zheng
zhenglichun@mail.ccmu.edu.cn

Beijing Luhe Hospital, Capital Medical University

Research Article

Keywords: SPECT/CT, MRI, Lacrimal gland, Thyroid-associated ophthalmopathy, Uptake ratio, Signal intensity ratio

Posted Date: November 18th, 2026

DOI: https://doi.org/10.21203/rs.3.rs-11570893/v1

License: This work is licensed under a Creative Commons Attribution 4.0 International License.
Read Full License

Additional Declarations: No competing interests reported.

Abstract

Purpose

To determine which quantitative lacrimal gland (LG) parameters from orbital MRI and 99mTc-DTPA SPECT/CT reflect thyroid-associated ophthalmopathy (TAO) activity once patient age is taken into account, and which are worth measuring in practice.

Methods

Forty-one patients with TAO (79 eyes) who had undergone 3T-MRI and SPECT/CT were studied retrospectively. Parameters were the signal intensity ratio of LG to white matter (SIR) and apparent diffusion coefficient (ADC) on MRI, and LG herniation (LGH) and uptake ratios (URs) on SPECT/CT. Activity was defined by a composite of the Clinical Activity Score (CAS), MRI and SPECT/CT. Each parameter was modelled crudely and then with adjustment for age; discrimination was assessed by the area under the curve (AUC), with DeLong's test.

Results

The groups differed in age (48.7 ± 12.8 vs 36.5 ± 8.2 years, P < 0.001), and age was itself associated with activity (odds ratio [OR] per 10 years = 3.04, 95% confidence interval [CI] 1.70–5.43; AUC = 0.775). SIR (OR = 22.0, P = 0.004), URcavg (OR = 1.74 per 0.1, P = 0.008) and LGH (OR = 1.39, P = 0.011) remained independent after adjustment. The combined SIR + URcavg model reached an AUC of 0.875 (95% CI 0.796–0.955), exceeding SIR alone (Z = 2.318, P = 0.020) and URcavg alone (Z = 2.436, P = 0.015); sensitivity was 91.3% and specificity 78.8%.

Conclusion

SIR and URcavg reflected TAO activity in a way the age difference between groups did not explain, and together they discriminated better than either did alone.

Introduction

Thyroid-associated ophthalmopathy (TAO), commonly referred to as Graves' ophthalmopathy, is a common autoimmune disorder of the orbit. Its inflammatory reactions produce proptosis, orbital fat infiltration and enlargement of the extraocular muscles and lacrimal glands [1, 2]. Both tissues express the thyroid-stimulating hormone receptor, and autoantibodies binding to it are thought to disrupt signalling and set off the inflammatory cascade. Activity determines whether a patient is offered immunosuppression or simply observed, and it is also the point at which imaging is most likely to change management.

Although the diagnosis of TAO traditionally focuses on the entire orbit, and particularly on the extraocular muscles, lacrimal gland involvement may be the presenting feature in a substantial proportion of patients [3]. The gland expresses the thyroid-stimulating hormone receptor on acinar and ductal cells, which makes it a direct immunological target rather than a passive bystander [4], and its involvement often precedes clinically evident muscle enlargement [3, 5]. Lying anterior to the orbital septum, it is readily and reproducibly delineated on both CT and MRI, and reduced tear secretion with ocular surface disease is a common although under-recognised complaint in TAO [3].

The Clinical Activity Score is the predominant method for evaluating activity, but its subjectivity is a significant limitation and several of its components derive from the inflammation it seeks to quantify [6]. MRI and SPECT/CT provide objective and complementary data [5, 7–10]: MRI reflects tissue water content and cellularity, whereas 99mTc-DTPA uptake reflects regional perfusion and tracer delivery. Which of these parameters carries information independent of patient age has not been settled, and the question matters because activity and age are frequently correlated in referral cohorts.

We quantified lacrimal gland parameters from SPECT/CT (URs, LGH) and 3T-MRI (SIR, ADC) in patients with TAO and identified those independently associated with activity after adjustment for age. A second aim was to compare the diagnostic performance of the parameters retained, individually and in combination. The study is distinguished by integrating quantitative metrics from both modalities.

Methods

Patients with TAO who underwent orbital MRI and 99mTc-DTPA SPECT/CT in the Departments of Radiology and Nuclear Medicine at our institution between January 2020 and February 2025 were reviewed retrospectively. Inclusion criteria were TAO diagnosed under the 2016 European Group on Graves' Orbitopathy (EUGOGO) guidelines [11], age over 18 years, and complete data from both modalities. Exclusion criteria were previous hormonal or surgical treatment for TAO or other causes of exophthalmos, pregnancy or lactation, no recorded CAS, an MRI protocol lacking the ADC sequence, and incomplete clinical records. The study was registered in the National Medical Research Registration and Filing Information System (www.medicalresearch.org.cn, registration number MR-11-26-010124).

Orbital SPECT/CT and MRI acquisition and clinical activity score

SPECT/CT was performed on a Symbia T16 system (Siemens, Germany) 20 minutes after administration of 99mTc-DTPA. Orbital MRI was performed on a 3.0-T scanner (uMR770/780, United Imaging, China) and comprised axial DWI, axial and coronal fat-suppressed T2-weighted images, axial and coronal T2-weighted images, and axial T1-weighted images, with ADC maps derived from b-values of 0 and 1000 s/mm². Imaging planes were parallel (axial, sagittal) or perpendicular (coronal) to the optic nerve. Acquisition parameters are given in the Supplementary Table.

Clinical activity was scored with the seven-point CAS recommended by EUGOGO at the initial visit by the ophthalmologist, covering conjunctival and eyelid oedema and redness, pain on eye movement, spontaneous retrobulbar pain, and inflammation of the caruncle or plica. A CAS of 3 or more indicated active TAO [12].

Diagnostic standard

For SPECT/CT analysis, the orbit was anatomically divided into retro-orbital (area posterior to the ocular equator) and pre-orbital (area anterior to the equator) regions, based on CT findings. Active inflammation was defined by elevated 99mTc-DTPA uptake in the retro-orbital region in contrast with adjacent brain tissue or in the pre-orbital area relative to adjacent skull bone [13].

On MRI, a T2 signal intensity (SI) greater in the EOMs than in the white matter (WM) or ipsilateral temporal muscle suggested active TAO [14]. A difference in T2 SI between the two eyes also indicated activity, the eye with the higher intensity being considered active. LG swelling with T2 hyperintensity was taken as further evidence of active disease [15, 16].

MRI, SPECT/CT and CAS were assessed within a short interval. The images were read independently by two experienced nuclear medicine physicians with consensus where readings differed, whereas the quantitative regions of interest were delineated by a single physician. An eye was classified as inactive when at least two of the three assessments were negative and as active when at least two were positive. Because CAS is one of the three components, it was never used as an independent gold standard; the composite classification was the outcome throughout.

Measurement

ROIs were drawn along the lacrimal gland contours on consecutive axial and coronal SPECT/CT slices showing the highest tracer uptake, excluding activity from the nasal cavity and skull. A reference ROI (R2) was placed on the occipital bone in a representative axial slice. Maximum and average counts were recorded for the glands (R1amax and R1aavg from axial slices, R1cmax and R1cavg from coronal slices) together with the maximum occipital count, and uptake ratios were calculated as R1/R2 (URamax, URaavg, URcmax, URcavg). Lacrimal gland herniation (LGH) was measured as the distance from the anterior aspect of the gland to the interzygomatic line.

In MRI, ROIs were identified on the T2WI FS and ADC axial images where the lacrimal gland demonstrated the highest SI. The ROI size was adjusted to encompass approximately 10–15% of the gland's cross-sectional area, as cited in existing literature [17–19]. The signal intensity ratio (SIR) was then calculated as the ratio of the SI of the lacrimal gland to that of the brain white matter.

Intra-observer reliability, assessed by re-measuring 11 randomly selected cases after at least two weeks, gave an intraclass correlation coefficient (ICC) of 0.86–0.99.

Statistical analysis

Continuous variables were summarized as mean ± SD or median (P25, P75), and compared with the t test or the Mann-Whitney U test; categorical variables were compared with the chi-square test, or with the Fisher exact test where expected counts were small. Spearman's coefficient was used for correlations.

Two features of the data required explicit handling. First, fellow eyes are not independent, so the primary analysis was performed at eye level (n = 79). Consistency was checked at patient level using one eye per patient, the eye with the higher SIR; 41 patients contributed 79 eyes. Second, the expected age difference could generate spurious associations, so age was treated as a prespecified confounder. The correlation of each parameter with age was quantified, univariable ORs were estimated crudely and with adjustment for age (per 10 years), URs being expressed per 0.1-unit increase, and age and sex were then entered together in a fully adjusted model.

The four UR indices were collinear (all pairwise rho ≥ 0.74) and could not be entered together; URcavg was chosen a priori as the coronal averaged metric, confirmed by stepwise selection with VIFs inspected in the final models. Diagnostic performance was assessed by ROC analysis, with Youden-optimal thresholds and the corresponding sensitivity, specificity, positive predictive value (PPV), negative predictive value (NPV) and accuracy. The AUC of the combined SIR + URcavg model was compared with those of the individual parameters by DeLong's test. Univariable and multivariable logistic regression yielded odds ratios (ORs) with 95% confidence intervals (CIs), and nested models were compared by likelihood ratio chi-square, AIC and BIC. There were no missing values among the parameters analysed, so no imputation was required. Two-sided $P < 0.05$ was considered significant, and analyses were performed in R 4.6.1 with the pROC package.

Results

Comparison between inactive and active TAO

Seventy-nine eyes from 41 patients met the eligibility criteria and were analyzed; 38 patients contributed both eyes and three contributed one. All quantitative parameters were higher in the active group (46 eyes) than in the inactive group (33 eyes) (Table 1).

Table 1
Comparison of quantitative parameters between active and inactive TAO eyes (eye level, n = 79)

Parameter	Inactive TAO	Active TAO	P value
SIR	0.93 ± 0.26	1.29 ± 0.37	< 0.001
ADC (×10 − 3 mm2/s)	1.23 (1.09, 1.30)	1.30 ± 0.10	0.010
LGH (mm)	13.31 ± 2.31	14.54 ± 2.68	0.032
URamax	1.15 (0.95, 1.61)	1.66 (1.38, 1.90)	0.001
URaavg	0.30 (0.25, 0.43)	0.46 (0.32, 0.68)	0.001
URcmax	1.08 (0.81, 1.50)	1.39 (1.10, 1.76)	0.008
URcavg	0.29 (0.24, 0.38)	0.45 (0.33, 0.59)	< 0.001
Age (years)	36.5 ± 8.2	48.7 ± 12.8	< 0.001
SIR: signal intensity ratio; ADC: apparent diffusion coefficient; LGH: lacrimal			
gland herniation; UR: uptake ratio.			

The two groups differed substantially in age (48.7 ± 12.8 vs 36.5 ± 8.2 years, P < 0.001). Age was itself strongly associated with activity (crude OR 3.04 per 10 years, 95% CI 1.70–5.43, P < 0.001; AUC = 0.775), and it was therefore treated as a potential confounder rather than a nuisance covariate.

Differences in TAO activity by sex and laterality

Activity did not differ between right and left eyes (χ^2 = 0.02, P = 0.894) but did differ between the sexes, being higher in males (χ^2 = 6.22, P = 0.013; continuity-corrected χ^2 = 5.13, P = 0.023; Fisher exact P = 0.022): 27 of 37 male eyes (73.0%) were active versus 19 of 42 female eyes (45.2%) (Table 2).

Table 2
Differences in TAO activity by sex and ocular laterality

Comparison	Inactive	Active	Pearson χ^2	P	Corrected χ^2	P	Fisher P
Right eye	16	23	0.02	0.894	0.00	1.000	1.000
Left eye	17	23	0.02	0.894	0.00	1.000	1.000
Female	23	19	6.22	0.013	5.13	0.023	0.022
Male	10	27	6.22	0.013	5.13	0.023	0.022
Each 2×2 block (right vs left eye; female vs male) shares one set of χ^2 and P values, repeated on both rows of the block. Corrected χ^2: continuity-corrected value.							

Correlation among parameters and with age

The four UR indices were highly intercorrelated (all pairwise rho ≥ 0.74) and carry largely the same information (Fig. 1). Their relationship with age was not uniform: LGH was independent of age (rho = 0.03, P = 0.79), whereas SIR (rho = 0.42), URcavg (rho = 0.34) and ADC (rho = 0.27) all increased with age (all P ≤ 0.015), so part of their crude difference may reflect the age structure of the groups rather than activity (Fig. 2; Supplementary Table S3).

Logistic regression: crude and age-adjusted associations

Every parameter was significantly associated with activity before adjustment. With age taken into account, SIR and three of the four UR indices remained significant, with attenuated but clearly preserved estimates: SIR adjusted OR = 22.04 (95% CI 2.72-178.46, P = 0.004), URcavg 1.74 (P = 0.008), URaavg 1.49 (P = 0.015) and URamax 1.13 (P = 0.033), whereas URcmax did not (1.10, 95% CI 0.99–1.23, P = 0.083) (Table 3).

Table 3
Univariable and multivariable logistic regression of TAO activity (eye level)

Parameter	Univariable logistic regression				Multivariable models			
	Crude OR (95% CI)	P	Age-adjusted OR (95% CI)	P	Model A OR (95% CI)	P	Model B OR (95% CI)	P
SIR	49.56 (6.35-386.94)	< 0.001	22.04 (2.72-178.46)	0.004	67.32 (6.22-728.96)	< 0.001	42.50 (3.11-580.04)	0.005
ADC	74.47 (1.54-3605.04)	0.029	14.52 (0.29-737.21)	0.182	—	—	—	—
LGH (mm)	1.21 (1.01–1.46)	0.041	1.39 (1.08–1.79)	0.011	—	—	—	—
URamax (per 0.1)	1.15 (1.04–1.27)	0.006	1.13 (1.01–1.26)	0.033	—	—	—	—
URaavg (per 0.1)	1.51 (1.14–1.99)	0.004	1.49 (1.08–2.06)	0.015	—	—	—	—
URcmax (per 0.1)	1.13 (1.02–1.25)	0.016	1.10 (0.99–1.23)	0.083	—	—	—	—
URcavg (per 0.1)	1.93 (1.31–2.84)	< 0.001	1.74 (1.15–2.64)	0.008	1.90 (1.26–2.86)	0.002	1.77 (1.19–2.64)	0.005
Age (per 10 years)	3.04 (1.70–5.43)	< 0.001	—	—	—	—	2.08 (1.02–4.22)	0.044
Male sex	—	—	—	—	—	—	2.51 (0.71–8.92)	0.154

Data are odds ratios (95% confidence intervals) from logistic regression with TAO activity (active vs inactive) as the dependent variable. SIR is an absolute ratio; ADC is in 10^{-3} mm²/s; UR is expressed per 0.1-unit increase; age is expressed per 10 years. Crude: each parameter entered alone. Age-adjusted: the parameter entered together with age. Model A contains SIR and URcavg, the four UR indices being collinear (all pairwise rho ≥ 0.74) and therefore not enterable together (McFadden R^2 = 0.346, AIC = 76.3, BIC = 83.4, AUC = 0.875); Model B adds age and sex (AIC = 71.8). SIR: signal intensity ratio; ADC: apparent diffusion coefficient; LGH: lacrimal gland herniation; UR: uptake ratio.

ADC and LGH moved in different directions. The crude OR of 74.47 for ADC (P = 0.029) fell to 14.52 once age was accounted for, and its confidence interval then spanned unity (95% CI 0.29-737.21, P = 0.182).

LGH rose: from 1.21 (P = 0.041) to 1.39 (95% CI 1.08–1.79, P = 0.011). It thus remained the only parameter whose odds ratio increased rather than attenuated once age was accounted for.

SIR and URcavg, entered together, were both independent predictors (SIR OR = 67.32, P < 0.001; URcavg OR = 1.90, P = 0.002; McFadden R^2 = 0.346). Adjustment for age and sex left both effects in place (SIR OR = 42.50, URcavg OR = 1.77, both P = 0.005); neither age (OR 2.08 per 10 years, P = 0.044) nor male sex (OR 2.51, P = 0.154) attenuated them materially, and VIFs of 1.01–1.08 excluded multicollinearity (Table 3). Adding URcavg to SIR improved the fit substantially (likelihood ratio chi-square = 14.53, P < 0.001), whereas adding age improved it only modestly and adding sex not at all (P = 0.149). LGH as a third term was small and imprecise (OR 1.10 per mm, 95% CI 0.86–1.39, P = 0.449) and raised both AIC (76.3 to 77.7) and BIC (83.4 to 87.2); the result was unchanged after further adjustment (OR 1.29, 95% CI 0.92–1.82, P = 0.147).

ROC analysis and DeLong's test

The AUCs of the individual parameters are shown in Fig. 3, ranging from 0.646 for LGH to 0.785 for SIR. The combined SIR + URcavg model performed better (AUC 0.875, 95% CI 0.796–0.955), with a sensitivity of 91.3% and a specificity of 78.8% at an optimal threshold probability of 0.44 (Fig. 4). DeLong's test did not separate the SIR and ADC curves (Z = 1.422, P = 0.155) or the SIR and LGH curves (Z = 1.691, P = 0.091).

DeLong's test confirmed the gain over SIR alone (Z = 2.318, P = 0.020) and URcavg alone (Z = 2.436, P = 0.015), whereas SIR and URcavg did not differ from each other (Z = 0.230, P = 0.818); the benefit thus arises from combining the modalities, not from superiority of either.

The Youden-optimal thresholds were SIR ≥ 1.11 and URcavg ≥ 0.41 (Table 4), with sensitivities of 0.652 and 0.609 and specificities of 0.788 and 0.879 respectively. Applied to the same eyes, the two rules agreed in only 48 of 79 eyes (61%; Cohen's kappa = 0.21).

Table 4
Youden-optimal thresholds and diagnostic performance (eye level)

Parameter	Cutoff	Sensitivity	Specificity	PPV	NPV	Accuracy	AUC (95% CI)
SIR	1.11	0.652	0.788	0.811	0.619	0.709	0.785 (0.686–0.885)
ADC	1.25	0.717	0.606	0.717	0.606	0.671	0.670 (0.543–0.797)
LGH (mm)	15.28	0.478	0.818	0.786	0.529	0.620	0.646 (0.525–0.767)
URamax	1.03	0.935	0.455	0.705	0.833	0.734	0.712 (0.592–0.832)
URaavg	0.30	0.826	0.515	0.704	0.680	0.696	0.713 (0.600-0.827)
URcmax	1.08	0.783	0.515	0.692	0.630	0.671	0.675 (0.553–0.798)
URcavg	0.41	0.609	0.879	0.875	0.617	0.722	0.768 (0.662–0.874)
Combined model	0.44*	0.913	0.788	0.857	0.867	0.861	0.875 (0.796–0.955)

*Threshold on the predicted probability from the logistic model. AUC: area under the receiver operating characteristic curve; PPV: positive predictive value; NPV: negative predictive value.

Sensitivity analysis at the patient level

With one eye per patient (n = 41; 24 active, 17 inactive), SIR remained higher in active patients (1.38 ± 0.35 vs 1.05 ± 0.19, P = 0.001) and the combined model retained comparable discrimination (AUC = 0.860). The eye-level findings were therefore not an artefact of correlated observations. Adjustment for age and sex left SIR independently predictive (OR 139.8, P = 0.037) but rendered URcavg non-significant (OR 1.50 per 0.1, P = 0.136), a loss of power consistent with the smaller sample rather than a contradiction of the main analysis.

Discussion

TAO is the most prevalent cause of orbital inflammation in adults and leads to expansion and proliferation of fibroblasts within the extraocular muscles and orbital fat [6, 20–22]. Imaging studies

have also identified symmetrical enlargement of the lacrimal glands as a secondary feature of TAO [23, 24]. Lacrimal gland enlargement is therefore a recognised marker of the disease, but its activity is better captured by more dynamic indices. Here we assessed TAO activity through lacrimal gland parameters obtained by SPECT/CT and MRI, which offers a different perspective on the same organ.

Diffusion-weighted imaging has diagnostic value in this setting, showing higher ADC values in the lacrimal glands of patients with TAO than in healthy volunteers. Razek et al. reported 1.83 ± 0.08 (1.62–1.92) × 10 − 3 mm2/s in active disease against 1.69 ± 0.04 (1.61–1.76) × 10 − 3 mm2/s in inactive disease [25], a difference attributed to mononuclear cell infiltration, fibroblast proliferation and oedema within the orbital tissues [26, 27]. Our data point in the same direction: lacrimal gland ADC was higher in active than in inactive eyes (1.30 ± 0.10 vs 1.23 [1.09–1.30] × 10 − 3 mm2/s, P = 0.010), though the absolute values were lower than those of Razek et al. [25]. Absolute ADC depends on field strength, b-value, ROI delineation and demographics, so cross-study comparison is of limited value. We therefore also calculated the SIR of the lacrimal gland to white matter, which is internally normalised and has shown superior diagnostic efficacy [28]. The AUC of SIR was 0.785, higher than that of ADC (0.670) but not significantly so (Z = 1.422, P = 0.155). SIR values referenced to extraocular muscle are remarkably consistent across studies [18, 19, 28], which indicates stability rather than superiority in discrimination. The preference for SIR rests less on its slightly higher AUC than on its behaviour after adjustment for age, considered below.

Age requires separate discussion, because the groups differed by twelve years (48.7 ± 12.8 vs 36.5 ± 8.2 years, P < 0.001) and age was itself a strong correlate of activity (crude OR 3.04 per 10 years, AUC 0.775), close to that of SIR (0.785). Any parameter correlated with age will therefore appear to mark activity in a cohort structured like ours, and three of the four did so: SIR (rho = 0.42), URcavg (rho = 0.34) and ADC (rho = 0.27) all rose with age and their crude estimates were correspondingly inflated. Adjustment attenuated SIR and URcavg substantially, from OR 49.6 to 22.0 and from 1.93 to 1.74, yet both remained clearly significant, so what they capture is not merely the age structure of the sample. ADC behaved differently: its crude OR of 74.5 collapsed to 14.5 with a confidence interval spanning unity, which suggests that much of its apparent association reflected age-related tissue change rather than inflammation. LGH moved in the opposite direction, rising from OR 1.21 to 1.39, and was the only parameter uncorrelated with age (rho = 0.03, P = 0.81). A similar independence has been reported for lacrimal gland dimensions in thyroid eye disease, where age did not determine gland enlargement [29]. In a cohort whose age distribution is uneven that is a property worth having, even though LGH did not add to a model already containing SIR and URcavg (P = 0.45).

Lacrimal gland SPECT/CT is a valuable tool for assessing inflammation and disease activity in TAO [7, 30, 31], and all UR values were higher in the active group in our cohort. This aligns with Jiang's findings on inflammatory infiltration in the extraocular muscles [32, 33], although only URcavg survived logistic regression here. The combination of SIR and URcavg reached an AUC of 0.875, slightly below the 0.89 and 0.91 reported for deep learning and radiomics applied to SPECT/CT in TAO activity [34, 35]. Manual delineation of UR and SIR may account for part of that gap. Those studies, however, addressed the

extraocular muscles and sometimes incorporated clinical indicators; to date no artificial intelligence study, machine learning or deep learning, has specifically targeted the lacrimal gland in TAO activity [36, 37].

This study has several limitations. First, it was single-centre and the sample was relatively small, so larger multicentre cohorts are needed. Second, all measurements were made by one observer and only intra-observer reliability was established, by re-measuring 11 randomly selected cases after at least two weeks (ICC 0.86–0.99); inter-observer variability was not addressed, and automated or semi-automated segmentation would reduce this source of bias. Third, activity was defined by a composite of CAS, MRI and SPECT/CT, and two of these three components derive from the imaging modalities under evaluation. Some circularity is therefore inherent in the reference standard, and our accuracy estimates should be read with that in mind; a definition resting on clinical criteria alone would avoid it. Fourth, the age imbalance arose from the referral pattern and could not be removed by design; adjustment addresses only measured confounding, and residual confounding by age-related orbital change cannot be excluded.

Conclusion

In conclusion, quantitative parameters of the lacrimal gland derived from orbital MRI and 99mTc-DTPA SPECT/CT hold significant value in evaluating TAO. Moreover, the integration of SPECT/CT and MRI enhances the diagnostic accuracy in assessing TAO activity. Of these parameters, SIR and URcavg remain independently predictive after adjustment for age and sex, whereas the association of ADC with activity is largely explained by age; LGH, being independent of age, may be less susceptible to confounding when the age distribution of a cohort is uneven.

Declarations

Competing interests The authors declare no competing interests.

Funding: None

Author Contributions

Lixin Sun contributed to the study conception and design. Material preparation and data collection were performed by Lixin Sun and Xin Ma. Data analysis was performed by Lixin Sun and Lichun Zheng. The first draft of the manuscript was written by Lixin Sun and all authors commented on previous versions of the manuscript. All authors read and approved the final manuscript.

Ethics approval and consent to participate: This study was approved by the Ethics Committee of Beijing Luhe Hospital, Capital Medical University (2025-LHKY-126-02), and the requirement to obtain written informed consent was waived.

Clinical trial number: not applicable

References

1. Bahn RS. Graves' ophthalmopathy. N Engl J Med. 2010;362:726–38.
2. Huh HD, Kim JH, Kim SJ, Yoo JM, Seo SW. The Change of Lacrimal Gland Volume in Korean Patients with Thyroid-associated Ophthalmopathy. Korean J Ophthalmol. 2016;30:319–25.
3. Selter JH, Gire AI, Sikder S. The relationship between Graves' ophthalmopathy and dry eye syndrome. Clin Ophthalmol. 2015;9:57–62.
4. Eckstein AK, Finkenrath A, Heiligenhaus A, Renzing-Köhler K, Esser J, Krüger C, Quadbeck B, Steuhl KP, Gieseler RK. Dry eye syndrome in thyroid-associated ophthalmopathy: lacrimal expression of TSH receptor suggests involvement of TSHR-specific autoantibodies. Acta Ophthalmol Scand. 2004;82:291–7.
5. Jiang M, Song X, Zhang H, Tao X, Yang G, Wang Y, Liu Y, Zhou H, Sun J, Li Y. The combination of T2-mapping value of lacrimal gland and clinical indicators can improve the stage prediction of Graves' ophthalmopathy compared to clinical activity scores. Endocrine. 2022;78:321–8.
6. Dolman PJ. Grading Severity and Activity in Thyroid Eye Disease. Ophthalmic Plast Reconstr Surg. 2018;34:S34–40.
7. Sun L, Peng R, Sun R. New Multi-Parameters Combination of Technetium-99m-Diethylene-Triamine-Pentaacetate Orbital Single-Photon Emission Computed Tomography/Computed Tomography for the Evaluation of Graves' Orbitopathy Activity. Semin Ophthalmol. 2024;39:387–93.
8. Kaichi Y, Tanitame K, Terada H, Itakura H, Ohno H, Yoneda M, Takahashi Y, Akiyama Y, Awai K. Thyroid-associated Orbitopathy: Quantitative Evaluation of the Orbital Fat Volume and Edema Using IDEAL-FSE. Eur J Radiol Open. 2019;6:182–6.
9. Chen L, Hu H, Chen HH, Chen W, Wu Q, Wu FY, Xu XQ. Usefulness of two-point Dixon T2-weighted imaging in thyroid-associated ophthalmopathy: comparison with conventional fat saturation imaging in fat suppression quality and staging performance. Br J Radiol. 2021;94:20200884.
10. Wu D, et al. Utility of multi-parametric quantitative magnetic resonance imaging of the lacrimal gland for diagnosing and staging Graves' ophthalmopathy. Eur J Radiol. 2021;141:109815.
11. Bartalena L, Baldeschi L, Boboridis K, Eckstein A, Kahaly GJ, Marcocci C, Perros P, Salvi M, Wiersinga WM. The 2016 European Thyroid Association/European Group on Graves' Orbitopathy Guidelines for the Management of Graves' Orbitopathy. Eur Thyroid J. 2016;5:9–26.
12. Bartalena L, Kahaly GJ, Baldeschi L, Dayan CM, Eckstein A, Marcocci C, Marinò M, Vaidya B, Wiersinga WM. The 2021 European Group on Graves' orbitopathy (EUGOGO) clinical practice guidelines for the medical management of Graves' orbitopathy. Eur J Endocrinol. 2021;185:G43–67.
13. Tang MT, Zeng XY, Li Y, Sun HT, Liu SY, Yuan X, Lu W. [The application of (99)Tc(m)-DTPA orbital SPECT/CT in staging evaluation of thyroid associated ophthalmopathy]. Zhonghua Yan Ke Za Zhi. 2021;57:830–6.
14. Liu X, et al. Application of Magnetic Resonance Imaging in the Evaluation of Disease Activity in Graves' Ophthalmopathy. Endocr Pract. 2021;27:198–205.

15. Gagliardo C, Radellini S, Morreale Bubella R, Falanga G, Richiusa P, Vadalà M, Ciresi A, Midiri M, Giordano C. Lacrimal gland herniation in Graves ophthalmopathy: a simple and useful MRI biomarker of disease activity. Eur Radiol. 2020;30:2138–41.
16. Huang D, Luo Q, Yang H, Mao Y. Changes of lacrimal gland and tear inflammatory cytokines in thyroid-associated ophthalmopathy. Invest Ophthalmol Vis Sci. 2014;55:4935–43.
17. Mayer EJ, Fox D, Herdman G, Hsuan J, Kabala J, Goddard P, Potts MJ, Lee RW. Signal intensity, clinical activity and cross-sectional areas on MRI scans in thyroid eye disease. Eur J Radiol. 2005;56:20–4.
18. Higashiyama T, Nishida Y, Morino K, Ugi S, Nishio Y, Maegawa H, Ohji M. Use of MRI signal intensity of extraocular muscles to evaluate methylprednisolone pulse therapy in thyroid-associated ophthalmopathy. Jpn J Ophthalmol. 2014;59:124–30.
19. Pajak M, Loba P, Wieczorek-Pastusiak J, Antosik-Biernacka A, Stefanczyk L, Majos A. Signal intensity and T2 time of extraocular muscles in assessment of their physiological status in MR imaging in healthy subjects. Pol J Radiol. 2012;77:7–12.
20. Baldeschi L, Wakelkamp IM, Lindeboom R, Prummel MF, Wiersinga WM. Early versus late orbital decompression in Graves' orbitopathy: a retrospective study in 125 patients. Ophthalmology. 2006;113:874–8.
21. Romero-Kusabara IL, Filho JV, Scalissi NM, Melo KC, Demartino G, Longui CA, Melo MR, Cury AN. Distinct inflammatory gene expression in extraocular muscle and fat from patients with Graves' orbitopathy. Eur J Endocrinol. 2017;176:481–8.
22. Pappa A, Calder V, Ajjan R, Fells P, Ludgate M, Weetman AP, Lightman S. Analysis of extraocular muscle-infiltrating T cells in thyroid-associated ophthalmopathy (TAO). Clin Exp Immunol. 1997;109:362–9.
23. Bingham CM, Harris MA, Realini T, Nguyen J, Hogg JP, Sivak-Callcott JA. Calculated computed tomography volumes of lacrimal glands and comparison to clinical findings in patients with thyroid eye disease. Ophthalmic Plast Reconstr Surg. 2014;30:116–8.
24. Harris MA, Realini T, Hogg JP, Sivak-Callcott JA. CT dimensions of the lacrimal gland in Graves orbitopathy. Ophthalmic Plast Reconstr Surg. 2012;28:69–72.
25. Razek AA, El-Hadidy EM, Moawad ME, El-Metwaly N, El-Said AA. Assessment of lacrimal glands in thyroid eye disease with diffusion-weighted magnetic resonance imaging. Pol J Radiol. 2019;84:e142–6.
26. Han JS, Seo HS, Lee YH, Lee H, Suh SI, Jeong EK, Sapkota N, Kim KJ. Fractional anisotropy and diffusivity changes in thyroid-associated orbitopathy. Neuroradiology. 2016;58:1189–96.
27. Feeney C, Lingam RK, Lee V, Rahman F, Nagendran S. Non-EPI-DWI for Detection, Disease Monitoring, and Clinical Decision-Making in Thyroid Eye Disease. AJNR Am J Neuroradiol. 2020;41:1466–72.
28. Sun AL, Peng R, Hao P. The value of signal intensity ratios of orbital tissue to white matter of orbital MRI in evaluating graves' orbitopathy. Int Ophthalmol. 2024;45:14.

29. Khan AM, Alawi A, Elkhamary SM, Sheikh O, Alsulaiman HM, Khandekar R, Schellini SA. Lacrimal gland enlargement in inactive thyroid eye disease: a case series and literature review. Arq Bras Oftalmol. 2025;88:e20240113.
30. Zhao RX, Shi TT, Luo S, Liu YF, Xin Z, Yang JK. The value of SPECT/CT imaging of lacrimal glands as a means of assessing the activity of Graves' orbitopathy. Endocr Connect. 2022;11:e210590.
31. Jiang C, Li X, Zhao M, Dend H, Huang J, Liu D, Xu X. Efficacy of 99mTc-DTPA orbital SPECT/CT on the evaluation of lacrimal gland inflammation in patients with thyroid associated ophthalmopathy. Zhong Nan Da Xue Xue Bao Yi Xue Ban. 2019;44:322–8.
32. Jiang C, Deng Z, Huang J, Deng H, Tan J, Li X, Zhao M. (2021) Monitoring and Predicting Treatment Response of Extraocular Muscles in Grave's Orbitopathy by (99m)Tc-DTPA SPECT/CT. Front Med (Lausanne) 8791131.
33. Liu D, Xu X, Wang S, Jiang C, Li X, Tan J, Deng Z. 99mTc-DTPA SPECT/CT provided guide on triamcinolone therapy in Graves' ophthalmopathy patients. Int Ophthalmol. 2020;40:553–61.
34. Yao N, et al. Deep learning-based diagnosis of disease activity in patients with Graves' orbitopathy using orbital SPECT/CT. Eur J Nucl Med Mol Imaging. 2023;50:3666–74.
35. Liu Y, et al. Diagnostic precision in thyroid-associated ophthalmopathy using multi-center radiomics with (99m)Tc-DTPA SPECT/CT. Sci Rep. 2024;14:25810.
36. Lin C, Song X, Li L, Li Y, Jiang M, Sun R, Zhou H, Fan X. Detection of active and inactive phases of thyroid-associated ophthalmopathy using deep convolutional neural network. BMC Ophthalmol. 2021;21:39.
37. Song X, Liu Z, Li L, Gao Z, Fan X, Zhai G, Zhou H. Artificial intelligence CT screening model for thyroid-associated ophthalmopathy and tests under clinical conditions. Int J Comput Assist Radiol Surg. 2020;16:323–30.

Figures

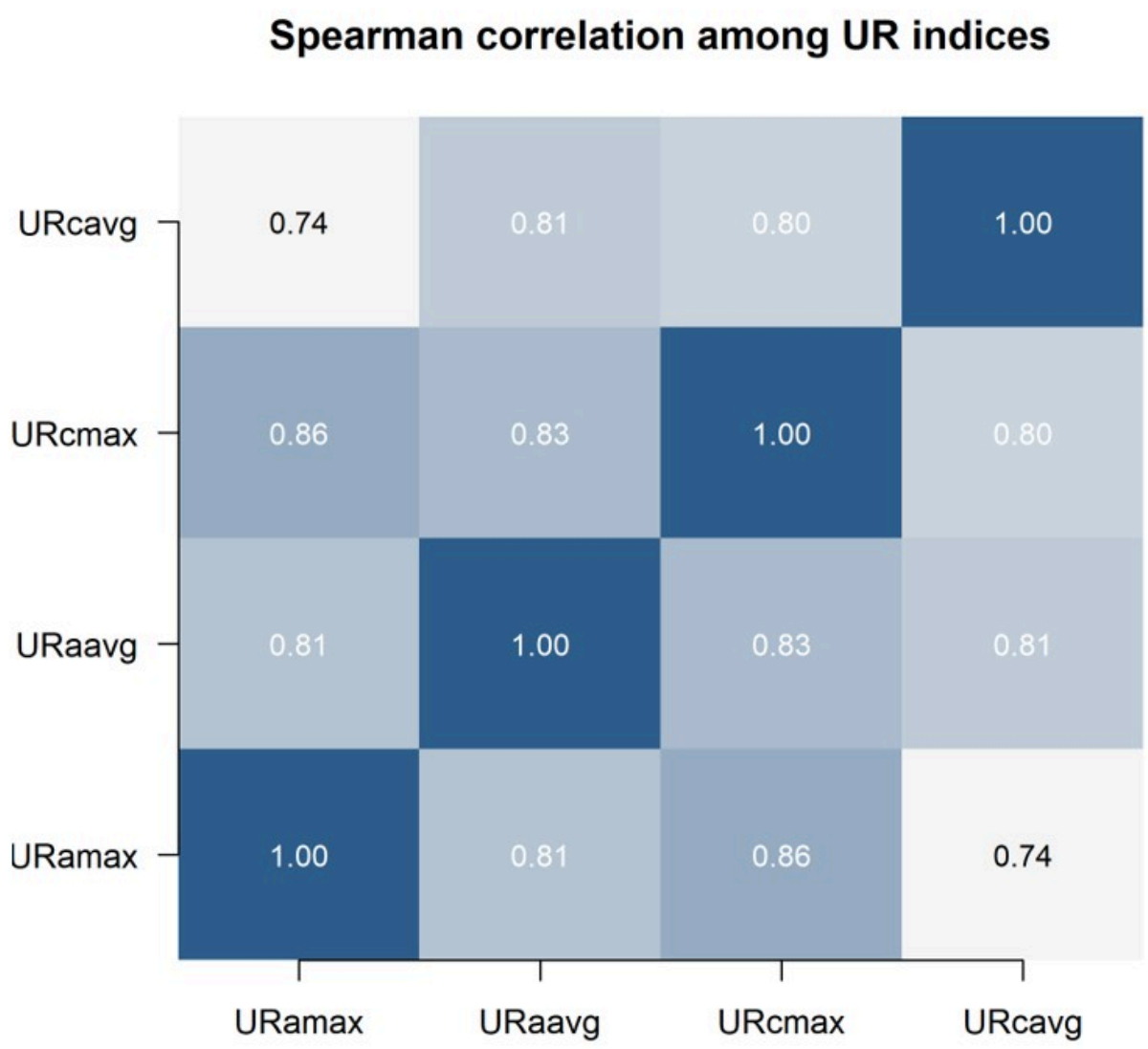


Figure 1

Correlation among the four uptake ratio indices (Spearman rank coefficient).

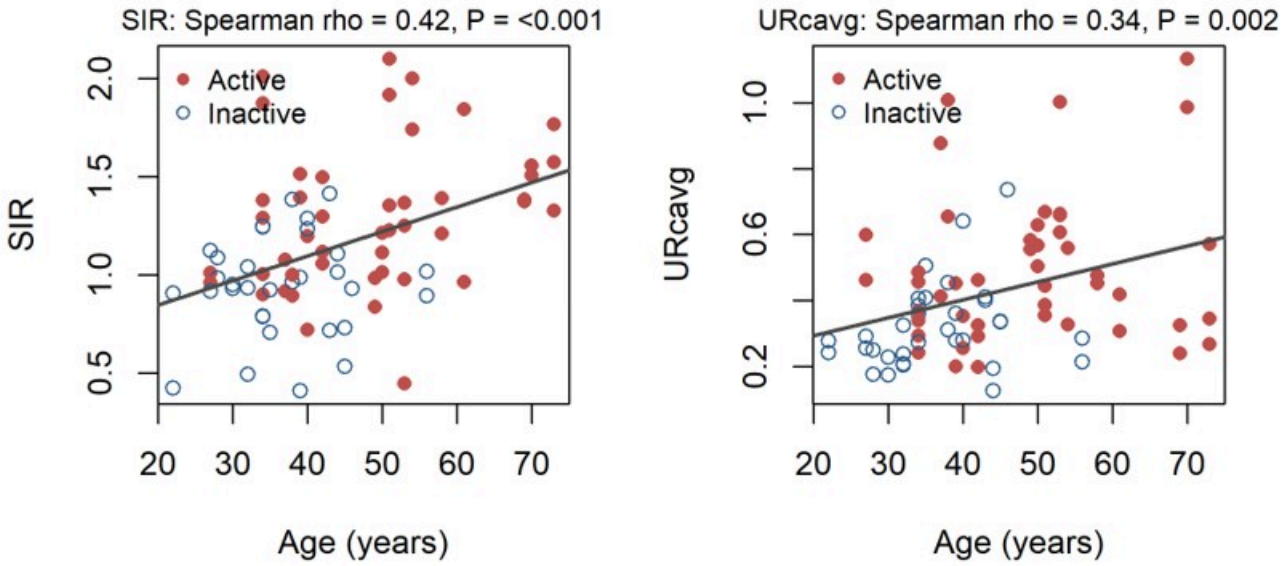


Figure 2

Age-related trends in the two principal parameters. SIR (left) and URcavg (right) are plotted against patient age; filled circles denote active and open circles inactive eyes, and the grey line is the univariable linear fit.

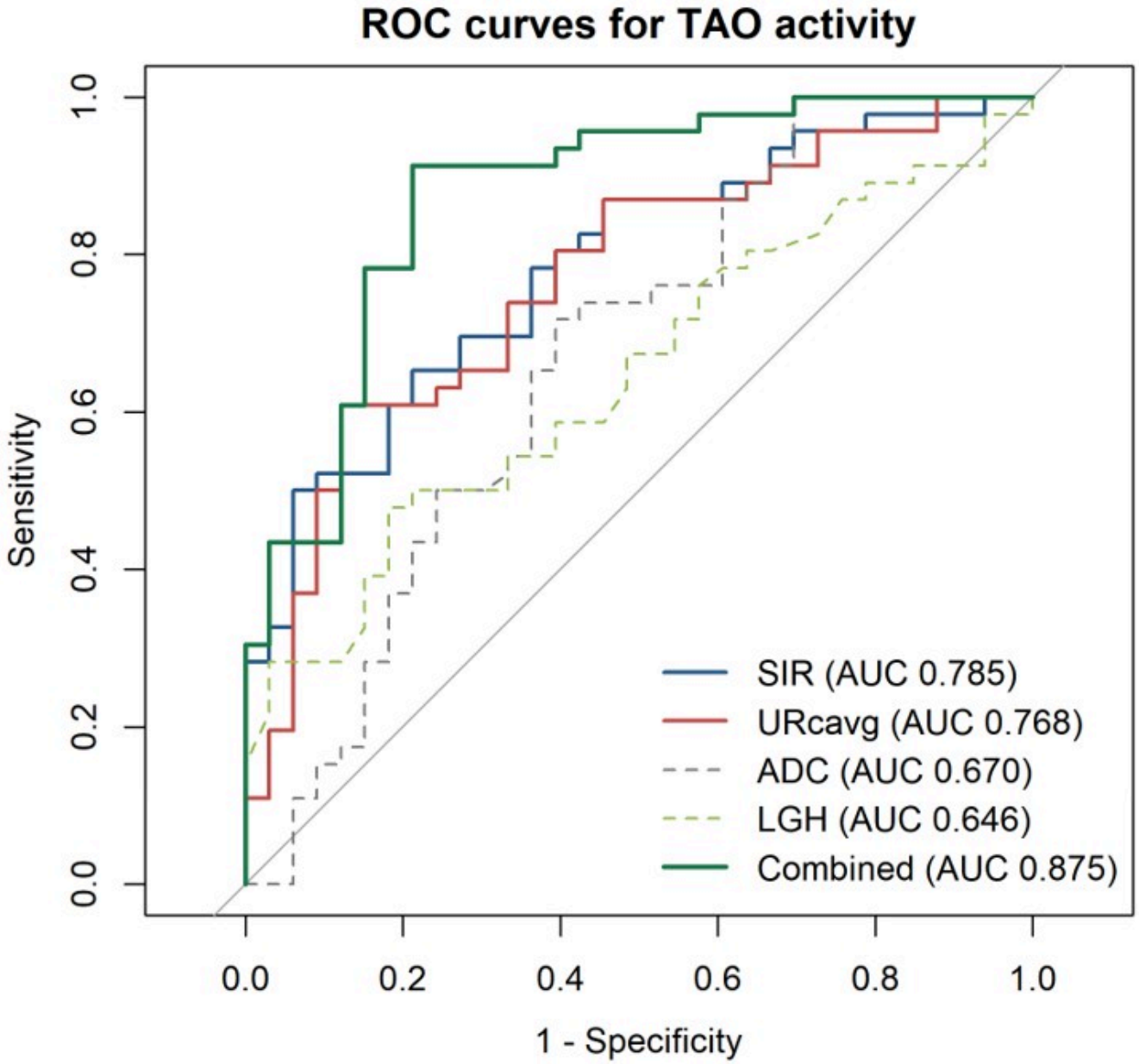


Figure 3

Receiver operating characteristic curves of individual parameters and of the combined SIR + URcavg model for TAO activity.

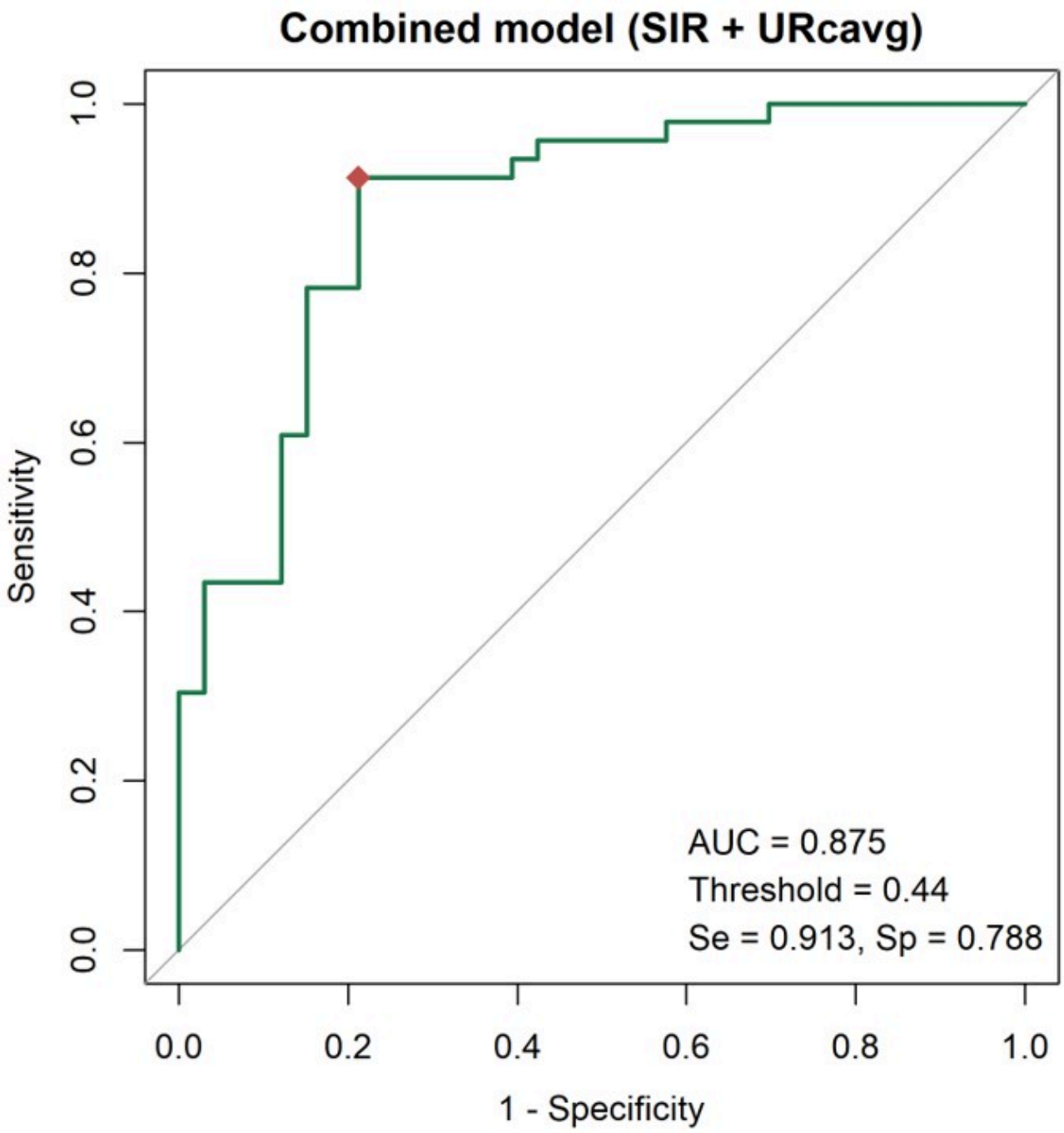


Figure 4

Receiver operating characteristic curve of the combined model with the optimal probability threshold, and the corresponding sensitivity and specificity.

Supplementary Files

This is a list of supplementary files associated with this preprint. Click to download.

- SupplementaryTable.docx